Analog Non-Linear Transformation-Based Tone Mapping for Image Enhancement in C-arm CT

Lan Shi, Martin Berger, Bastian Bier, Christopher Soell, Juergen Roeber,
Rebecca Fahrig, Bjoern Eskofier, Andreas Maier, Jennifer Maier

***Abstract*—Flat-Panel C-arm Computed Tomography (CT) suffers from pixel saturation due to the detector's limited dynamic range. We describe a novel approach of analog, non-linear tone mapping (TM) for preventing detector saturation. An analog TM operator (TMO) applies a non-linear transformation in a CMOS (complementary metal-oxide semiconductor) sensor and its inverse TMO based on 14-bit digital raw data. This is done in order to prevent overexposure and to enhance image quality to 32 bits. The method was applied to the cases of low-contrast head imaging and to that of imaging both knees. Cone-beam projection data with and without overexposure was simulated for a 200 degree short-scan of the knees and a 360 degree full-scan of a Forbild head phantom. The results show an increased correlation coefficient with respect to ground truth of 0.99 for TMO compared to 0.96 for overexposed knee data and a higher low-contrast visibility (CC=0.99) compared to linear quantization (CC=0.97).**

I. Introduction

Cone-beam C-arm computed tomography (CT) systems equipped with flat panel detectors are used to acquire 3D CT images with high spatial resolution. Advantages compared to clinical CT scanners are their versatile positioning and ability to record a volume scan in one sweep [1].

The dynamic range of current flat panel detectors is often limited to 14 bits, which can lead to saturation of the photo diodes [2]. In order to ensure the visibility of dense tissue a high dose is applied, which leads to the overexposure of less dense material, introducing artifacts similar to truncation [3]. An application suffering from this is imaging both knee joints for cartilage deformation analysis. Due to the geometry of the knees, overexposure primarily occurs at the peripheral leg boundary, and is currently avoided by adding absorbing material around the knees [4].

Another well-known problem is the low-contrast visibility when C-arm CTs conduct scans of the head. As opposed to clinical scanners, C-arm CT's low-contrast visibility is much lower [2]. Reasons for this are the detector's limited bit depth, and increased x-ray scatter and more image noise generated by the cone-beam geometry [3]. It has been shown that low-contrast detectability can be improved by deliberate overexposure [2]. This again leads to saturation causing truncation-like artifacts.

J. Maier, M. Berger, B. Bier, B. Eskofier and A. Maier are with the Department of Computer Science, Pattern Recognition Lab, L. Shi, C. Soell and J. Roeber are with the Department of Electrical Engineering, Institute for Electronics Engineering, Friedrich-Alexander-University Erlangen-Nuremberg, Germany. R. Fahrig is with the Radiological Sciences Laboratory, Stanford University, CA, now with Siemens Healthcare GmbH.

Corresponding author: jennifer.maier@fau.de

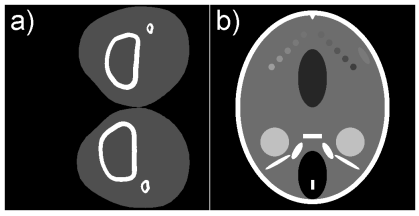

Fig. 1. Axial slices of simulated volume data: a) tibia and fibula below the knee, b) Forbild head phantom with low contrast spheres

We propose a novel tone mapping (TM) method, which transforms the intensities prior to discretization in the analog domain, such that overexposure can be avoided.

II. Methods

A. Data Simulation

To analyze the issues of overexposure and low-contrast visibility, we simulated cone-beam CT projection data of knees and a Forbild head phantom. The detector for the knee simulation had a size of 620 x 480 pixels and rotated 200° around the objects creating 248 projections, which is comparable to actual short-scan data acquisition. For the head, the detector had 640 x 480 pixels and recorded 512 projections on a 360° full-scan. In both cases, the energy spectrum was monochromatic at 55 keV.

The simulated head scan data was a modified Forbild phantom. Similar to Knaup et al. [2], we added eight 4 mm low-contrast spheres in the posterior brain region. Compared to the 50 Hounsfield Unit (HU) brain matter, they had a contrast of ± 5, ± 10, ± 15 and ± 20 HU. For the knee scan simulation, we created a phantom that contains the femur, tibia, fibula and patella, and skin material around the bones [5].

We rendered the volume as well as the projections for both phantoms. One slice of each volume is shown in Figure 1.

B. Overexposure Simulation

Detector saturation was simulated to mimic overexposure. The intensities in the attenuation projection images were normalized between 0 and 1, where unattenuated beams created a value of 1. To simulate overexposure, all values above 0.35 were set to 0.35.

C. Non-linear Transformation

We propose an image processing pipeline connected with a CMOS (complementary metal-oxide semiconductor) sensor

array, as depicted in Figure 2. It contains an analog TM operator (TMO) to create a non-linear transformation of the intensity curve and avoid saturation, a 14-bit analog-digital-converter (ADC), and a digital inverse TMO to obtain the full intensity range of the detector for reconstruction. By these means, a 3D-reconstruction with an approximated high dynamic range (HDR) image quality can be achieved, although the detector is limited to 14-bit low dynamic range (LDR) raw data.

The analog TMO is introduced in [6]. It is a global algorithm based on Reinhard's method *Photographic Tone Reproduction* (PTR) [7] and can be described as follows:

$$q_T(x,y,z) = f_{TMO}(q_H, \mu_a)$$
$$= V_a \frac{\kappa_a \cdot q_H(x,y,z) + q_H(x,y,z)^2 \cdot P_\mu \cdot \mu_a(z) \cdot P_w}{\kappa_a \cdot q_H(x,y,z) + P_\mu \cdot \mu_a(z)}$$

where $q_H(x,y,z)$ is the detected sensor pixel intensity of row x, column y and frame z; $\mu_a(z)$ is the average value of each frame according to charge compensation principle; V_a is the sensor effective range; $P_w = 1/q_{max}^2$; $P_\mu = mean(\mu_g(z)/\mu_a(z))$ scales the arithmetic mean μ_a to the geometric mean μ_g; κ_a is the brightness control key (standard values: 0.09, 0.18, 0.36, 0.72) [7]. The key is chosen based on whether the scene is low-key (dark, high contrast) or high-key (bright, low contrast).

In our simulation, the input signals $q_H(x,y,z)$, $\mu_a(z)$ and all parameters are floating data in the range of $[0,1]$. Assuming $V_a = 1$, $q_{max} = 1$, P_μ is calibrated with the simulated cone-beam CT projection data. $\kappa_a = 0.72$ was chosen for this case.

The 14-bit ADC quantizes the tone mapped sensor signal $q_T(x,y,z)$. The LDR output $q_L(x,y,z)$ is simulated as the 14-bit detector raw data with an additional output $\mu_a(z)$ for each frame. Based on both sensor output signals, an inverse function $q'_H(x,y,z) = f_{TMO}^{-1}(q_L, \mu_a)$ is solved for a positive result at 32 bits to improve the image quality.

D. Reconstruction

To correct for the truncation-like artifacts resulting from overexposure, a water cylinder truncation correction was applied to the overexposed projections before reconstruction [2].

The projections were reconstructed through filtered back-projection (cosine weighting, Parker weighting for short-scan, Shepp-Logan ramp). The reconstructed volumes had a size of 512x512x512 for the head scan and only 512x512x256 for the knee scan with an isotropic voxel size of 0.5mm.

III. Results

Figure 3 shows the reconstructions of the knee's ground truth projections (3a), overexposed and truncation corrected projections (3b), and tone mapped projections (3c). The correlation coefficient (CC) between the ground truth and overexposed reconstruction is 0.96, whereas the CC for the tone mapped reconstruction increased to 0.99.

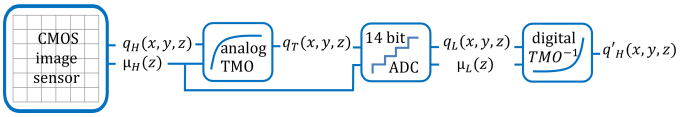

Fig. 2. Proposed image processing pipeline for non-linear transformations

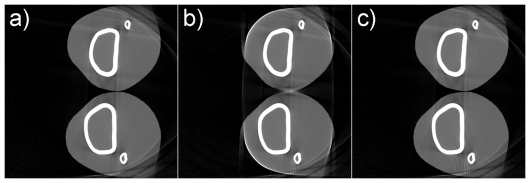

Fig. 3. Reconstructions of the processed knee projections, slice 60. a) ground truth, b) overexposed (CC = 0.96), c) non-linear tone mapped (CC=0.99)

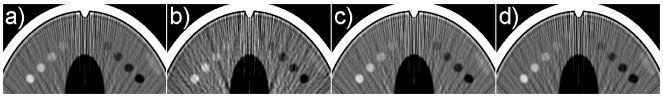

Fig. 4. Reconstructions of the processed head projections, slice 256. a) ground truth, b) 14-bit linear quantized (CC=0.97), c) overexposed (CC=0.99), d) non-linear tone mapped (CC=0.99)

In Figure 4, the image region of the head reconstruction containing the low-contrast spheres is shown, blurred with a Gaussian kernel of σ. Compared to the ground truth (4a), only 6 spheres are plainly visible in the 14-bit linear quantized image (4b). For deliberate overexposure (4c) as well as for the tone-mapped data (4d), all spheres can clearly be seen. The CC of the image region compared to ground truth is 0.97 for linear quantization, and 0.99 for overexposure and TMO.

IV. Discussion and Conclusion

We presented a method for reducing overexposure artifacts and for improving low-contrast visibility by applying an analog non-linear transformation.

In the overexposed knee reconstructions, the skin boundary between the legs is blurred and the front of the knees is cropped. The water cylinder correction did not work well for these projections, because the scanned object resembles two water cylinders rather than one. Preuhs [8] developed an optimization-based multiple-cylinder fitting to solve this issue, which only works for perfect cylinder-like objects. The TMO was able to restore all skin borders. These findings are confirmed by the higher CC for TMO. If our method were to be implemented on the detector, the additional absorbing material in [4] could be spared, thus improving patient comfort and clinical applicability.

Truncation corrected overexposure and tone mapping achieve comparable results for the head data, which shows that TMO can be used instead of the former method.

For the applications presented above, we have shown that tone mapping can prevent detector saturation and enhance low-contrast visibility. The method was purely a simulation and only tested on simulated data. In future work, the analog TMO and 14-bit ADC will be combined in an ADC design with a 14-bit, tone-mapped curve to directly improve the image sensor performance for medical applications.

REFERENCES

[1] D. A. Jaffray and J. H. Siewerdsen, "Cone-beam computed tomography with a flat-panel imager: initial performance characterization." *Medical physics*, vol. 27, no. 6, pp. 1311–23, jun 2000.

[2] M. Knaup *et al.*, "Digitization and visibility issues in flat detector CT: A simulation study," in *2012 IEEE Nuclear Science Symposium and Medical Imaging Conference Record (NSS/MIC)*. IEEE, oct 2012, pp. 2661–2666.

[3] M. Zellerhoff *et al.*, "Low contrast 3D-reconstruction from C-arm data," in *Progress in Biomedical Optics and Imaging - Proceedings of SPIE*, M. J. Flynn, Ed., vol. 5745, no. I, apr 2005, pp. 646–655.

[4] J.-H. Choi *et al.*, "Fiducial marker-based correction for involuntary motion in weight-bearing C-arm CT scanning of knees. II. Experiment." *Medical physics*, vol. 41, no. 6, p. 061902, jun 2014.

[5] W. P. Segars *et al.*, "4d xcat phantom for multimodality imaging research," *Medical Physics*, vol. 37, no. 9, p. 4902, 2010.

[6] L. Shi *et al.*, "A Tone Mapping Algorithm Suited for Analog-Signal Real-Time Image Processing," in *12th International Conference on PhD Research in Microelectronics and Electronics (PRIME)*, Lisbon, Portugal, jun 2016.

[7] E. Reinhard *et al.*, "Photographic Tone Reproduction for Digital Images," *ACM Trans. Graph.*, vol. 21, no. 3, pp. 267–276, Jul. 2002.

[8] A. Preuhs *et al.*, "Over-Exposure Correction in CT Using Optimization-Based Multiple Cylinder Fitting," in *Bildverarbeitung für die Medizin 2015*. Springer Berlin Heidelberg, jan 2015, pp. 35–40.